

1-1-2006

# Optimal Therapy Regimens for Treatment-Resistant Mutations of HIV

Weiqing Gu  
*Harvey Mudd College*

Helen Moore  
*American Institute of Mathematics*

---

## Recommended Citation

Gu, Weiqing; Moore, Helen. "Optimal therapy regimens for treatment-resistant mutations of HIV." *Mathematical studies on human disease dynamics*, 139–152, *Contemp. Math.*, 410, Amer. Math. Soc., Providence, RI, 2006.

This Book Chapter is brought to you for free and open access by the HMC Faculty Scholarship at Scholarship @ Claremont. It has been accepted for inclusion in All HMC Faculty Publications and Research by an authorized administrator of Scholarship @ Claremont. For more information, please contact [scholarship@cuc.claremont.edu](mailto:scholarship@cuc.claremont.edu).

## Optimal therapy regimens for treatment-resistant mutations of HIV

Weiqing Gu and Helen Moore

**ABSTRACT.** In this paper, we use control theory to determine optimal treatment regimens for HIV patients, taking into account treatment-resistant mutations of the virus. We perform optimal control analysis on a model developed previously for the dynamics of HIV with strains of various resistance to treatment (Moore and Gu, 2005). This model incorporates three types of resistance to treatments: strains that are not responsive to protease inhibitors, strains not responsive to reverse transcriptase inhibitors, and strains not responsive to either of these treatments. We solve for the optimal treatment regimens analytically and numerically. We find parameter regimes for which optimal dosing is substantially better than constant dosing, but we also find parameter regimes for which optimal dosing is only marginally better than constant dosing. We propose the following open problem: Classify the settings in which variable-dose regimens determined by optimal control methods yield significantly better outcomes than comparable constant-dose regimens.

### 1. Introduction

Over 40 million people worldwide are estimated to be living with human immunodeficiency virus (HIV) [30]. Progression from HIV infection to acquired immunodeficiency syndrome (AIDS) typically occurs over a decade or two. In 2005, over three million people died from AIDS; since the first cases were identified in 1981, over 25 million have died from AIDS [30]. The immune system and, in particular, the T cells, play a central role in HIV population dynamics, including the progression to AIDS [33, 5]. There are various treatments in use, but no available treatment protocol results in documented complete clearance of the virus from patients. Current drug treatments are able to extend the healthy life span of infected patients by years.

One of the main problems in controlling the virus is the emergence of drug-resistant strains of HIV in patients undergoing treatment [28]. These mutant strains result in the resurgence of viral loads after long-term suppression of virus during

---

2000 *Mathematics Subject Classification.* Primary 49K15; Secondary 34, 92.

*Key words and phrases.* Human immunodeficiency virus (HIV), differential equations, dynamics, mathematical modeling, optimal control, T cells, treatment-resistant mutations.

Gu's work was supported in part by NSF DMS Grant 041401.

Moore's work was supported in part by NSF DMS Grant 0111966.

treatment. Viral load resurgence correlates with T cell depletion, and the progression of patients to AIDS [33]. In this paper, we apply mathematical modeling and analysis techniques to examine the properties of a model that includes drug-resistant strains. We use control theory to optimize treatment regimes in this setting, with the goal of maintaining patient health (as measured by T cell count) for as long as possible.

We begin with the differential equation model of T cell interaction with HIV in Moore and Gu [18]. There is an extensive body of work which develops models of this type for the interaction of T cells with HIV. Perelson and Nelson [25] and Nowak and May [23] have written detailed surveys of the main ideas developed through such models. Several other diseases with similar pathogen-immune system interaction dynamics have been modeled in this way as well. These include hepatitis B (cf. [21]), hepatitis C (cf. [20]), tuberculosis (cf. [34]) and chronic myelogenous leukemia (CML) (cf. [19]).

Most relevant to the specific model we present here are the models of HIV that incorporate drug-resistant strains of HIV. Such models include those of McLean et al. [15], Nowak et al. [22], McLean and Nowak [16], Frost and McLean [9], Kirschner and Webb [13], De Boer and Boucher [4], Goudsmit et al. [10], Wein et al. [32], Wein et al. [31], Stilianakis et al. [29], Bonhoeffer and Nowak [2], and Bonhoeffer et al. [1, 3].

Among the previous models that have considered mutant strains of HIV, most have considered only a single drug-resistant strain. One contribution of the model of Moore and Gu is the analysis of a model with three different drug-resistant strains: one strain resistant to treatment in the protease inhibitor (PI) class, one resistant to treatment in the reverse transcriptase inhibitor (RTI) class, and one resistant to treatment in both classes. In the current paper, we apply control theory to this model with two drug treatments, one a PI and one an RTI. We solve for the optimal dosing regimens, with the PI and RTI dosages allowed to be independent. Some earlier work applying optimal control to HIV, for example, the papers by Kirschner et al. [12] and Fister et al. [7], considered latently infected T cell populations (which we do not consider here), but did not examine drug-resistant strains.

We present both analytical and numerical results in this paper, solving for the optimal treatment regimens. In the numerical work, we compare variable dosing computed using optimal control with constant dosing that uses the same total amount of drug over the treatment period. We find parameter regimes for which optimal dosing is superior to the comparable constant dosing, but we also find parameter regimes for which optimal dosing is only marginally better than constant dosing. We believe that characterizations distinguishing the two cases are an important goal, with clinical implications for the use of optimal control to develop new drug dosing protocols.

## 2. Details and explanation of the model

See [18] for more background and justification of the original model. Note that the model is valid only for certain parameter ranges. The reference [18] discusses some of the necessary restrictions on parameter values. Here we include only the information necessary to complete our optimal control analysis. We consider five populations of T cells in the circulating blood system. The first is the population

of T cells which is uninfected with any HIV. The other four are T cells that are infected with various populations of HIV, as described below. The T cell populations infected with different HIV strains are indexed using binary notation. Quantities related to wild-type, drug-sensitive HIV have the subscript “00”, those related to strains resistant to the PI have the subscript “01”, those related to strains resistant to the RTI have the subscript “10”, and those related to strains resistant to both drugs have the subscript “11”.

We assume that the various viral strains are at or near equilibrium. This allows us to avoid additional equations for free virus, since we approximate free virus populations as being proportional to populations of T cells infected with the corresponding strains.

All cell populations are measured in concentrations of cells per  $\mu\text{l}$ , and are functions of time,  $t$ , which is measured in days:

$$\begin{aligned} T &= \text{uninfected T cells,} \\ I_{00} &= \text{T cells with drug-sensitive wild-type virus,} \\ I_{01} &= \text{T cells with virus with mutations of type 1 and not of type 2,} \\ I_{10} &= \text{T cells with virus with mutations of type 2 and not of type 1,} \\ I_{11} &= \text{T cells with virus with mutations of types 1 and 2.} \end{aligned}$$

The basic model with treatment is shown below, followed by brief explanations of the terms:

$$\begin{aligned} \frac{dT}{dt} &= s + pT \left( 1 - \frac{T + I_{00} + I_{01} + I_{10} + I_{11}}{T_{\max}} \right) - \delta_T T \\ (2.1) \quad &- [(1 - \eta_2)\beta_{00}I_{00} + (1 - \eta_2)\beta_{01}I_{01} + \beta_{10}I_{10} + \beta_{11}I_{11}] T \\ \frac{dI_{00}}{dt} &= (1 - \eta_2)\beta_{00}I_{00}T - \delta_{00}I_{00} + (1 - \eta_1)\kappa_{00}(1 - \mu_{01})(1 - \mu_{10})I_{00} \\ (2.2) \quad &+ \kappa_{01}\bar{\mu}_{10}(1 - \mu_{10})I_{01} + (1 - \eta_1)\kappa_{10}(1 - \mu_{01})\bar{\mu}_{10}I_{10} + \kappa_{11}\bar{\mu}_{01}\bar{\mu}_{10}I_{11} \\ \frac{dI_{01}}{dt} &= (1 - \eta_2)\beta_{01}I_{01}T - \delta_{01}I_{01} + \kappa_{01}(1 - \bar{\mu}_{01})(1 - \mu_{10})I_{01} \\ (2.3) \quad &+ (1 - \eta_1)\kappa_{00}\mu_{01}(1 - \mu_{10})I_{00} + (1 - \eta_1)\kappa_{10}\mu_{01}\bar{\mu}_{10}I_{10} + \kappa_{11}(1 - \bar{\mu}_{01})\bar{\mu}_{10}I_{11} \\ \frac{dI_{10}}{dt} &= \beta_{10}I_{10}T - \delta_{10}I_{10} + (1 - \eta_1)\kappa_{10}(1 - \mu_{01})(1 - \bar{\mu}_{10})I_{10} \\ (2.4) \quad &+ (1 - \eta_1)\kappa_{00}(1 - \mu_{01})\mu_{10}I_{00} + \kappa_{01}\bar{\mu}_{01}\mu_{10}I_{01} + \kappa_{11}\bar{\mu}_{01}(1 - \bar{\mu}_{10})I_{11} \\ \frac{dI_{11}}{dt} &= \beta_{11}I_{11}T - \delta_{11}I_{11} + \kappa_{11}(1 - \bar{\mu}_{01})(1 - \bar{\mu}_{10})I_{11} \\ (2.5) \quad &+ (1 - \eta_1)\kappa_{00}\mu_{01}\mu_{10}I_{00} + \kappa_{01}(1 - \bar{\mu}_{01})\mu_{10}I_{01} + (1 - \eta_1)\kappa_{10}\mu_{01}(1 - \bar{\mu}_{10})I_{10} \end{aligned}$$

Each equation represents the rate of change, with respect to time, of one of the populations. The lowercase coefficients, or parameters, (e.g.,  $s$  and  $\mu_{01}$ ) are all taken to be constants, as is  $T_{\max}$ .

The first term on the right-hand side of equation (2.1) is a constant source term,  $s$ , for new T cells entering the blood system. The second term is a growth term, with logistic growth rate  $p$  and limiting value  $T_{\max}$ . We use all of the T cell populations considered here (uninfected and infected with HIV) in the logistic population count. The third term is the loss due to the natural attrition of  $T$  population cells, with death rate constant  $\delta_T$ .

The last four terms in equation (2.1) represent losses of healthy T cells from the peripheral blood due to interaction and subsequent infection with various types of HIV. Each of these terms is in mass action form, as they represent contributions due to encounters between T cells and HIV occurring in the peripheral blood, which we assume is well-mixed. Recall that we are assuming that the concentration of free virus of each type is proportional to the concentration of T cells infected with each type of HIV. Hence  $\beta_{ij}I_{ij}$  includes a constant of proportionality that gives the concentration of free virus of type  $ij$ , as well as the law of mass action constant, which incorporates the expected frequency of encounters between T cells and HIV, and the expected fraction of these encounters that subsequently lead to infection by HIV.

We now examine the four equations (2.2)–(2.5), which describe the rates of change of T cells infected with the four types of strains of HIV we consider here. In each of these equations, the first term is a contribution that equals a loss term for T cells in equation (2.1). For example, in equation (2.2), the first term is equal to the rate of loss of T cells which become infected by wild-type HIV. The second term in each of the four equations is a loss term  $\delta_{ij}I_{ij}$  due to the natural life span of T cells, with  $\delta_{ij}$  the death rate constant for T cells infected with HIV of type  $ij$ . We assume that  $\delta_{ij}$  is at least as large as the death rate of healthy T cells,  $\delta_T$ .

The constants  $\mu_{ij}$ , for  $ij = 01$  and  $ij = 10$ , give the average mutation frequencies for the mutations that lead to HIV with mutations of type 1 and type 2, respectively. These mutations are assumed to be independent, and hence the mutation frequency for HIV with mutations of both type 1 and type 2 is given by  $\mu_{01}\mu_{10}$ . The factors  $(1 - \mu_{01})$  and  $(1 - \mu_{10})$  give the fractions of virus that are expected to not mutate to strains of type 1 or type 2, respectively, at any given time. The constants  $\bar{\mu}_{ij}$ , for  $ij = 01$  or  $ij = 10$  represent the corresponding backward mutation frequencies. For example,  $\bar{\mu}_{01}$  represents the mutation frequency of strains of type 1 back to wild-type virus.

The constants  $\kappa_{ij}$  are the net gain scaling factors, or effective virus release rate constants. As an example, the term  $\kappa_{00}(1 - \mu_{01})(1 - \mu_{10})I_{00}$  in equation (2.2) gives the contribution to the  $I_{00}$  population due to release of virions from the infected T cells  $I_{00}$  that do not mutate to one of the other types of strains considered here. Similarly, the term  $\kappa_{01}\bar{\mu}_{01}I_{01}$  in equation (2.2) gives the contribution to the  $I_{00}$  population due to release of virions from the infected T cells  $I_{01}$  that mutate from strains of type 1 back to wild-type virus. We point out that in the previously published model [18], terms such as  $\kappa_{01}\bar{\mu}_{01}(1 - \mu_{10})I_{01}$  in equation (2.2) were approximated by  $\kappa_{01}\bar{\mu}_{01}I_{01}$ , but we do not make such approximations in this paper.

We let  $\eta_1$  denote the efficacy of treatment with a protease inhibitor (PI), and let  $\eta_2$  denote the efficacy of treatment with a reverse transcriptase inhibitor (RTI), where  $0 \leq \eta_1 \leq 1$  and  $0 \leq \eta_2 \leq 1$ , with 0 corresponding to no treatment and 1 corresponding to treatment that is 100% efficacious. Recall that  $I_{01}$  is the population that is resistant only to the PI,  $I_{10}$  is resistant only to the RTI, and  $I_{11}$  is resistant to both treatments. Since RTIs block new infection, the factor  $(1 - \eta_2)$  appears in terms for new infections coming from the healthy T cell population, and gives the fraction of those new infections that are not blocked by the RTI. The factor does not appear in terms representing new infections by virus that is resistant to RTI. Since PIs block the production of new virions, the factor  $(1 - \eta_1)$  appears in terms for the production of new virus, and gives the fraction of production that is

not blocked by the PI. Any production that is not blocked then has the chance to mutate.

### 3. Optimal control analysis

We define the objective functional as

$$(3.1) \quad J(\eta_1, \eta_2) = \int_{t_{\text{initial}}}^{t_{\text{final}}} \left[ T(t) - (w_{00}I_{00}(t) + w_{01}I_{01}(t) + w_{10}I_{10}(t) + w_{11}I_{11}(t)) - \frac{1}{2}B_1\eta_1^2(t) - \frac{1}{2}B_2\eta_2^2(t) \right] dt$$

where  $w_{ij}$  and  $B_k$  are positive weighting constants for  $i, j = 0, 1, k = 1, 2$ . We wish to maximize  $J(\eta_1, \eta_2)$  for the state equations (2.1)–(2.5). The objective functional includes the integral of  $T$  since one measure of patient health is T cell count, and explicitly including this term helps maintain the healthy T cell counts over the treatment period. The homeostatic form of equation (2.1) does not allow this term to be too large at any time, and so it cannot completely compensate for the effect of high doses of chemotherapy. The functional includes penalty terms for infected populations, since it will be detrimental for the patient at later times to have developed resistant populations. We set  $w_{00} < w_{01}$ ,  $w_{00} < w_{10}$ ,  $w_{01} < w_{11}$ , and  $w_{10} < w_{11}$ , since we want most to minimize  $I_{11}$ , then  $I_{01}$  and  $I_{10}$ , and to yet a lesser extent,  $I_{00}$ . The last two terms in the integrand take into account the detrimental effect of chemotherapy on patient health. This effect is expected to be nonlinear, and we use the simplest nonlinear functions of  $\eta_1$  and  $\eta_2$ , as in [12].

The admissible set of control functions is

$$(3.2) \quad \mathcal{U}(t) = \{(\eta_1(t), \eta_2(t)) \mid \eta_k(t) \text{ Lebesgue measurable, } 0 \leq \eta_k(t) \leq 1, k = 1, 2\}.$$

We define the Hamiltonian  $H$  to be

$$(3.3) \quad \begin{aligned} H = & T - (w_{00}I_{00}(t) + w_{01}I_{01}(t) + w_{10}I_{10}(t) + w_{11}I_{11}(t)) - \frac{1}{2}B_1\eta_1^2 - \frac{1}{2}B_2\eta_2^2 \\ & + \lambda_1 \left[ s + pT \left( 1 - \frac{T + I_{00} + I_{01} + I_{10} + I_{11}}{T_{\text{max}}} \right) - \delta_T T \right. \\ & \left. - ((1 - \eta_2)\beta_{00}I_{00} + (1 - \eta_2)\beta_{01}I_{01} + \beta_{10}I_{10} + \beta_{11}I_{11}) T \right] \\ & + \lambda_2 [(1 - \eta_2)\beta_{00}I_{00}T - \delta_{00}I_{00} + (1 - \eta_1)\kappa_{00}(1 - \mu_{01})(1 - \mu_{10})I_{00} \\ & + \kappa_{01}\bar{\mu}_{01}(1 - \mu_{10})I_{01} + (1 - \eta_1)\kappa_{10}(1 - \mu_{01})\bar{\mu}_{10}I_{10} + \kappa_{11}\bar{\mu}_{01}\bar{\mu}_{10}I_{11}] \\ & + \lambda_3 [(1 - \eta_2)\beta_{01}I_{01}T - \delta_{01}I_{01} + \kappa_{01}(1 - \bar{\mu}_{01})(1 - \mu_{10})I_{01} \\ & + (1 - \eta_1)\kappa_{00}\mu_{01}(1 - \mu_{10})I_{00} + (1 - \eta_1)\kappa_{10}\mu_{01}\bar{\mu}_{10}I_{10} + \kappa_{11}(1 - \bar{\mu}_{01})\bar{\mu}_{10}I_{11}] \\ & + \lambda_4 [\beta_{10}I_{10}T - \delta_{10}I_{10} + (1 - \eta_1)\kappa_{10}(1 - \mu_{01})(1 - \bar{\mu}_{10})I_{10} \\ & + (1 - \eta_1)\kappa_{00}(1 - \mu_{01})\mu_{10}I_{00} + \kappa_{01}\bar{\mu}_{01}\mu_{10}I_{01} + \kappa_{11}\bar{\mu}_{01}(1 - \bar{\mu}_{10})I_{11}] \\ & + \lambda_5 [\beta_{11}I_{11}T - \delta_{11}I_{11} + \kappa_{11}(1 - \bar{\mu}_{01})(1 - \bar{\mu}_{10})I_{11} \\ & + (1 - \eta_1)\kappa_{00}\mu_{01}\mu_{10}I_{00} + \kappa_{01}(1 - \bar{\mu}_{01})\mu_{10}I_{01} + (1 - \eta_1)\kappa_{10}\mu_{01}(1 - \bar{\mu}_{10})I_{10}] . \end{aligned}$$

By the Pontryagin Maximum Principle (cf. [8]), there exist adjoint variables  $\lambda_1, \lambda_2, \lambda_3, \lambda_4, \lambda_5$  satisfying the following:

$$\begin{aligned} \frac{d\lambda_1}{dt} &= -\frac{\partial H}{\partial T} \\ &= -\left\{1 + \lambda_1 \left[ p \left( 1 - \frac{T + I_{00} + I_{01} + I_{10} + I_{11}}{T_{\max}} \right) - p \frac{T}{T_{\max}} - \delta_T \right. \right. \\ &\quad \left. \left. - ((1 - \eta_2)\beta_{00}I_{00} + (1 - \eta_2)\beta_{01}I_{01} + \beta_{10}I_{10} + \beta_{11}I_{11}) \right] \right. \\ (3.4) \quad &\left. + \lambda_2(1 - \eta_2)\beta_{00}I_{00} + \lambda_3(1 - \eta_2)\beta_{01}I_{01} + \lambda_4\beta_{10}I_{10} + \lambda_5\beta_{11}I_{11} \right\}, \end{aligned}$$

$$\begin{aligned} \frac{d\lambda_2}{dt} &= -\frac{\partial H}{\partial I_{00}} \\ &= -\left\{ -w_{00} + \lambda_1 \left[ -p \frac{T}{T_{\max}} - (1 - \eta_2)\beta_{00}T \right] \right. \\ &\quad \left. + \lambda_2 [(1 - \eta_2)\beta_{00}T - \delta_{00} + (1 - \eta_1)\kappa_{00}(1 - \mu_{01})(1 - \mu_{10})] \right. \\ &\quad \left. + \lambda_3(1 - \eta_1)\kappa_{00}\mu_{01}(1 - \mu_{10}) \right. \\ (3.5) \quad &\left. + \lambda_4(1 - \eta_1)\kappa_{00}(1 - \mu_{01})\mu_{10} + \lambda_5(1 - \eta_1)\kappa_{00}\mu_{01}\mu_{10} \right\}, \end{aligned}$$

$$\begin{aligned} \frac{d\lambda_3}{dt} &= -\frac{\partial H}{\partial I_{01}} \\ &= -\left\{ -w_{01} + \lambda_1 \left[ -p \frac{T}{T_{\max}} - (1 - \eta_2)\beta_{01}T \right] + \lambda_2\kappa_{01}\bar{\mu}_{01}(1 - \mu_{10}) \right. \\ &\quad \left. + \lambda_3 [(1 - \eta_2)\beta_{01}T - \delta_{01} + \kappa_{01}(1 - \bar{\mu}_{01})(1 - \mu_{10})] \right. \\ (3.6) \quad &\left. + \lambda_4\kappa_{01}\bar{\mu}_{01}\mu_{10} + \lambda_5\kappa_{01}(1 - \bar{\mu}_{01})\mu_{10} \right\}, \end{aligned}$$

$$\begin{aligned} \frac{d\lambda_4}{dt} &= -\frac{\partial H}{\partial I_{10}} \\ &= -\left\{ -w_{10} + \lambda_1 \left[ -p \frac{T}{T_{\max}} - \beta_{10}T \right] + \lambda_2(1 - \eta_1)\kappa_{10}(1 - \mu_{01})\bar{\mu}_{10} \right. \\ &\quad \left. + \lambda_3(1 - \eta_1)\kappa_{10}\mu_{01}\bar{\mu}_{10} + \lambda_4 [\beta_{10}T - \delta_{10} + (1 - \eta_1)\kappa_{10}(1 - \mu_{01})(1 - \bar{\mu}_{10})] \right. \\ (3.7) \quad &\left. + \lambda_5(1 - \eta_1)\kappa_{10}\mu_{01}(1 - \bar{\mu}_{10}) \right\}, \end{aligned}$$

$$\begin{aligned} \frac{d\lambda_5}{dt} &= -\frac{\partial H}{\partial I_{11}} \\ &= -\left\{ -w_{11} + \lambda_1 \left[ -p \frac{T}{T_{\max}} - \beta_{11}T \right] + \lambda_2\kappa_{11}\bar{\mu}_{01}\bar{\mu}_{10} + \lambda_3\kappa_{11}(1 - \bar{\mu}_{01})\bar{\mu}_{10} \right. \\ (3.8) \quad &\left. + \lambda_4\kappa_{11}\bar{\mu}_{01}(1 - \bar{\mu}_{10}) + \lambda_5 [\beta_{11}T - \delta_{11} + \kappa_{11}(1 - \bar{\mu}_{01})(1 - \bar{\mu}_{10})] \right\}, \end{aligned}$$

where  $\lambda_k(t_{\text{final}}) = 0$  for  $k = 1, 2, 3, 4, 5$  are the transversality conditions.

We next compute  $\frac{\partial H}{\partial \eta_1}$  and  $\frac{\partial H}{\partial \eta_2}$ :

$$\begin{aligned} \frac{\partial H}{\partial \eta_1} &= -B_1\eta_1 - \lambda_2 [\kappa_{00}(1 - \mu_{01})(1 - \mu_{10})I_{00} + \kappa_{10}(1 - \mu_{01})\bar{\mu}_{10}I_{10}] \\ &\quad - \lambda_3 [\kappa_{00}\mu_{01}(1 - \mu_{10})I_{00} + \kappa_{10}\mu_{01}\bar{\mu}_{10}I_{10}] \\ &\quad - \lambda_4 [\kappa_{10}(1 - \mu_{01})(1 - \bar{\mu}_{10})I_{10} + \kappa_{00}(1 - \mu_{01})\mu_{10}I_{00}] \\ (3.9) \quad &\quad - \lambda_5 [\kappa_{00}\mu_{01}\mu_{10}I_{00} + \kappa_{10}\mu_{01}(1 - \bar{\mu}_{10})I_{10}], \end{aligned}$$

$$(3.10) \quad \frac{\partial H}{\partial \eta_2} = -B_2\eta_2 + \lambda_1 [\beta_{00}I_{00}T + \beta_{01}I_{01}T] - \lambda_2\beta_{00}I_{00}T - \lambda_3\beta_{01}I_{01}T.$$

At an optimal solution  $\vec{\eta}^*(t) = (\eta_1^*(t), \eta_2^*(t))$  in the interior of  $\mathcal{U}$ , we have  $\frac{\partial H}{\partial \eta_1} = 0$  and  $\frac{\partial H}{\partial \eta_2} = 0$ , so the optimal solution in our setting is given by the equations below, with the additional constraints that  $0 \leq \eta_k \leq 1$  for  $k = 1, 2$ :

$$\begin{aligned} \eta_1 = & -\frac{1}{B_1} \{ \lambda_2 [\kappa_{00}(1 - \mu_{01})(1 - \mu_{10})I_{00} + \kappa_{10}(1 - \mu_{01})\bar{\mu}_{10}I_{10}] \\ & + \lambda_3 [\kappa_{00}\mu_{01}(1 - \mu_{10})I_{00} + \kappa_{10}\mu_{01}\bar{\mu}_{10}I_{10}] \\ & + \lambda_4 [\kappa_{10}(1 - \mu_{01})(1 - \bar{\mu}_{10})I_{10} + \kappa_{00}(1 - \mu_{01})\mu_{10}I_{00}] \\ & + \lambda_5 [\kappa_{00}\mu_{01}\mu_{10}I_{00} + \kappa_{10}\mu_{01}(1 - \bar{\mu}_{10})I_{10}] \}, \end{aligned} \quad (3.11)$$

$$\eta_2 = \frac{1}{B_2} \{ \lambda_1 [\beta_{00}I_{00}T + \beta_{01}I_{01}T] - \lambda_2\beta_{00}I_{00}T - \lambda_3\beta_{01}I_{01}T \}. \quad (3.12)$$

#### 4. Existence and uniqueness of the optimal solution

We obtain existence of the optimal control solution  $\vec{\eta}^* = (\eta_1^*, \eta_2^*)$  by applying a result such as Theorem 4.1 in section III.4 of [8]. This theorem applies to our model because the set  $\mathcal{U}$  is compact and the integrand of the functional  $J$  is convex in  $\vec{\eta}$ . The uniqueness of the optimal solution  $\vec{\eta}^*$  for sufficiently small  $t_{\text{final}} - t_{\text{initial}}$  follows by using some of the same types of estimates as those in Theorem 4.1 of [7], so we do not include the calculations here. The bound  $T \leq T_{\text{max}}$  implies the needed bounds on  $I_{ij}$  for  $i, j = 0, 1$  and on  $\lambda_i$  for  $i = 1, 2, 3, 4, 5$  for  $t_{\text{final}} - t_{\text{initial}}$  sufficiently small.

### 5. Numerical results

**5.1. Background information.** In this section, we compute numerical solutions to the system in equations (2.1) - (2.5) under various treatment scenarios. For all of these computations, we use code we wrote in Mathematica<sup>TM</sup> 5.0. For the optimal control solutions, we start with initial values for the cell populations and initial guesses for each of the drug regimens. We calculate the cell populations on the entire time interval by using a fourth-order Runge-Kutta method to numerically solve equations (2.1) - (2.5). We then use these populations and the final time values of the adjoint variables to solve for the adjoint variables from equations (3.4) - (3.5), on the entire time interval. The calculated cell populations and adjoint variables are used in (3.11) - (3.12) to update  $\eta_1$  and  $\eta_2$ . We iterate this forward-backward scheme to move toward the optimal control solutions for the drug regimens, and the resulting cell populations. See [11] for a previously-published example of this method.

The values of the constants used to solve the systems of differential equations are as shown in Table 1, unless otherwise noted. The table gives a brief description of the constants, the values used as estimates for the constants, and any units and references for the constants.

We use the following initial values for the populations, where  $t = 0$  is the starting time for the model, and the units are cells/ $\mu\text{l}$ :  $T(0) = 1200$ ,  $I_{00}(0) = 20$ ,  $I_{01}(0) = 5$ ,  $I_{10}(0) = 5$ ,  $I_{11}(0) = 2$ .

For reference, in Figure 1 we show graphs of the solution curves to equations (2.1)–(2.5), but with no treatment ( $\eta_1 = \eta_2 = 0$ ). The parameter values are those that appear in Table 1. We see that T cells infected with the wild-type virus dominate all others, and approach a positive stable equilibrium value.



TABLE 1. Parameter information.

Param.	Description	Value	Units	Ref.
$s$	$T$ source term	0.048	$\frac{\text{cells}/\mu\text{l}}{\text{day}}$	[17]
$p$	$T$ logistic rate constant	0.0045	$\text{day}^{-1}$	[31], [24]
$T_{\max}$	maximum $T$	2000	$\text{cells}/\mu\text{l}$	[17]
$\delta_T$	$T$ death rate constant	0.0014	$\text{day}^{-1}$	[31]
$\delta_{00}$	$I_{00}$ death rate constant	0.45	$\text{day}^{-1}$	[26]
$\delta_{01}$	$I_{01}$ death rate constant	0.5	$\text{day}^{-1}$	est.
$\delta_{10}$	$I_{10}$ death rate constant	0.5	$\text{day}^{-1}$	est.
$\delta_{11}$	$I_{11}$ death rate constant	0.55	$\text{day}^{-1}$	est.
$\beta_{00}$	$I_{00}$ proport./mass act./infect.	$3 \times 10^{-4}$	$\frac{\text{day}^{-1}}{\text{cells}/\mu\text{l}}$	[31], [6]
$\beta_{01}$	$I_{01}$ proport./mass act./infect.	$2.8 \times 10^{-4}$	$\frac{\text{day}^{-1}}{\text{cells}/\mu\text{l}}$	est.
$\beta_{10}$	$I_{10}$ proport./mass act./infect.	$2.8 \times 10^{-4}$	$\frac{\text{day}^{-1}}{\text{cells}/\mu\text{l}}$	est.
$\beta_{11}$	$I_{11}$ proport./mass act./infect.	$2.5 \times 10^{-4}$	$\frac{\text{day}^{-1}}{\text{cells}/\mu\text{l}}$	est.
$\kappa_{00}$	$I_{00}$ effective burst rate const.	0.45	$\frac{\text{day}^{-1}}{\text{cells}/\mu\text{l}}$	est.
$\kappa_{01}$	$I_{01}$ effective burst rate const.	0.42	$\frac{\text{day}^{-1}}{\text{cells}/\mu\text{l}}$	est.
$\kappa_{10}$	$I_{10}$ effective burst rate const.	0.42	$\frac{\text{day}^{-1}}{\text{cells}/\mu\text{l}}$	est.
$\kappa_{11}$	$I_{11}$ effective burst rate const.	0.41	$\frac{\text{day}^{-1}}{\text{cells}/\mu\text{l}}$	est.
$\mu_{01}$	frequency of mutation to type 1	$2.5 \times 10^{-5}$	—	est.
$\mu_{10}$	frequency of mutation to type 2	$3 \times 10^{-5}$	—	[14]
$\bar{\mu}_{01}$	freq. of mut. away from type 1	$2.5 \times 10^{-5}$	—	est.
$\bar{\mu}_{10}$	freq. of mut. away from type 2	$3 \times 10^{-5}$	—	est.
$w_{00}$	weight for $I_{00}$ term	10	—	est.
$w_{01}$	weight for $I_{01}$ term	100	—	est.
$w_{10}$	weight for $I_{10}$ term	100	—	est.
$w_{11}$	weight for $I_{11}$ term	1000	—	est.
$B_1$	severity weight for $\eta_1$	100	—	est.
$B_2$	severity weight for $\eta_2$	200	—	est.

**5.2. Optimal control treatment vs. constant-dose treatment.** To compare constant doses with variable doses computed using optimal control, we used doses with the same total amount of each drug. That is, the integral of each drug level is the same for the two different regimens over the time period considered. In this initial work, we examined relatively short time periods. We were easily able to find parameters for which we observed variable drug dosing computed using optimal control was superior or comparable to the corresponding constant-dose regimens.

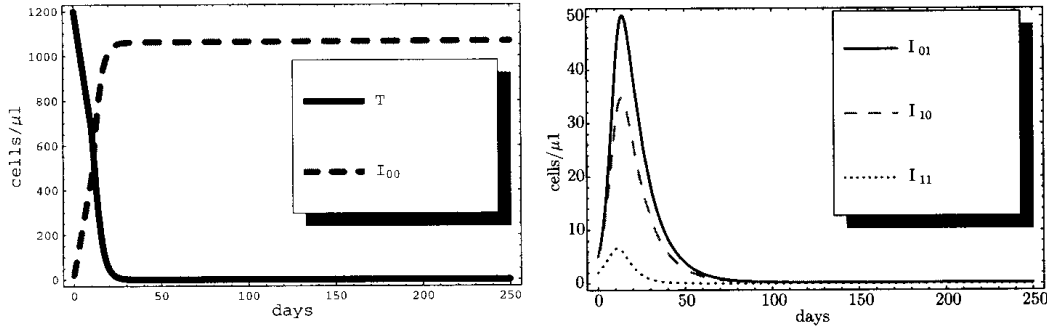


FIGURE 1. Qualitative T cell population behavior in the absence of treatment. Uninfected T cells are shown in black, T cells infected with wild-type virus are shown in purple, T cells infected with strains resistant to type 1 treatment are blue, resistant to type 2 treatment are green, and resistant to both types of treatments are red. Cells per  $\mu\text{l}$  are on the vertical axis, days are on the horizontal axis, for this and all following graphs.

We show examples of each in Figures 2 and 3: one in which optimal control dosing substantially outperforms a constant-dose regimen with the same total amount of drugs, and one in which the difference between the two regimens is marginal. Table 2 gives any parameter values that differ from those listed in Table 1.

Since the T cell populations infected with HIV are driven to very low numbers in all of our examples on the time scale considered here, we use uninfected T cell counts as a measure of patient health. We especially consider the threshold of 200 healthy T cells per  $\mu\text{l}$ , as T cell counts below 200 cells/ $\mu\text{l}$  are commonly considered to be the hallmark of progression to AIDS. In Figure 2, the variable-dose regimen obtained from optimal control gives substantially better results than the comparable constant-dose regimen. At the end of the 250-day time period, the variable-dose regimen yields a healthy T cell count of approximately 334 cells/ $\mu\text{l}$ , and the constant-dose regimen yields a healthy T cell count of approximately 237 cells/ $\mu\text{l}$ . The variable-dose regimen also keeps these T cell counts above 200/ $\mu\text{l}$  for the entire time period, while the constant-dose regimen shows counts that dip below this mark. In Figure 3, neither drug dosing protocol leads to healthy T cell counts below 200 cells/ $\mu\text{l}$ , and the healthy T cell counts at the end of the 250-day period are approximately 334 and 322 cells/ $\mu\text{l}$  for variable dosing and constant dosing, respectively.

In both scenarios, the optimal solution drug doses are initially at their maxima. This can be attributed to the fact that the treatment begins after the patient has had the infection for a period of time, and has a T cell count that is below normal levels [18]. Numerical results in [12] give a graphical demonstration of this effect for a similar system. The optimal doses appear to monotonically decrease because our objective contains a penalty for the total amount of drug applied, but also rewards high T cell counts over time. This reward results in a higher optimal drug dose earlier in the time period, due to the benefit to  $T$ . Higher drug doses mean reduced loss of  $T$  and reduced gain of  $I_{ij}$  for  $i, j = 0, 1$ . Because the objective is an integral over time, the time involved in the transition between  $T$  and  $I_{ij}$  (which

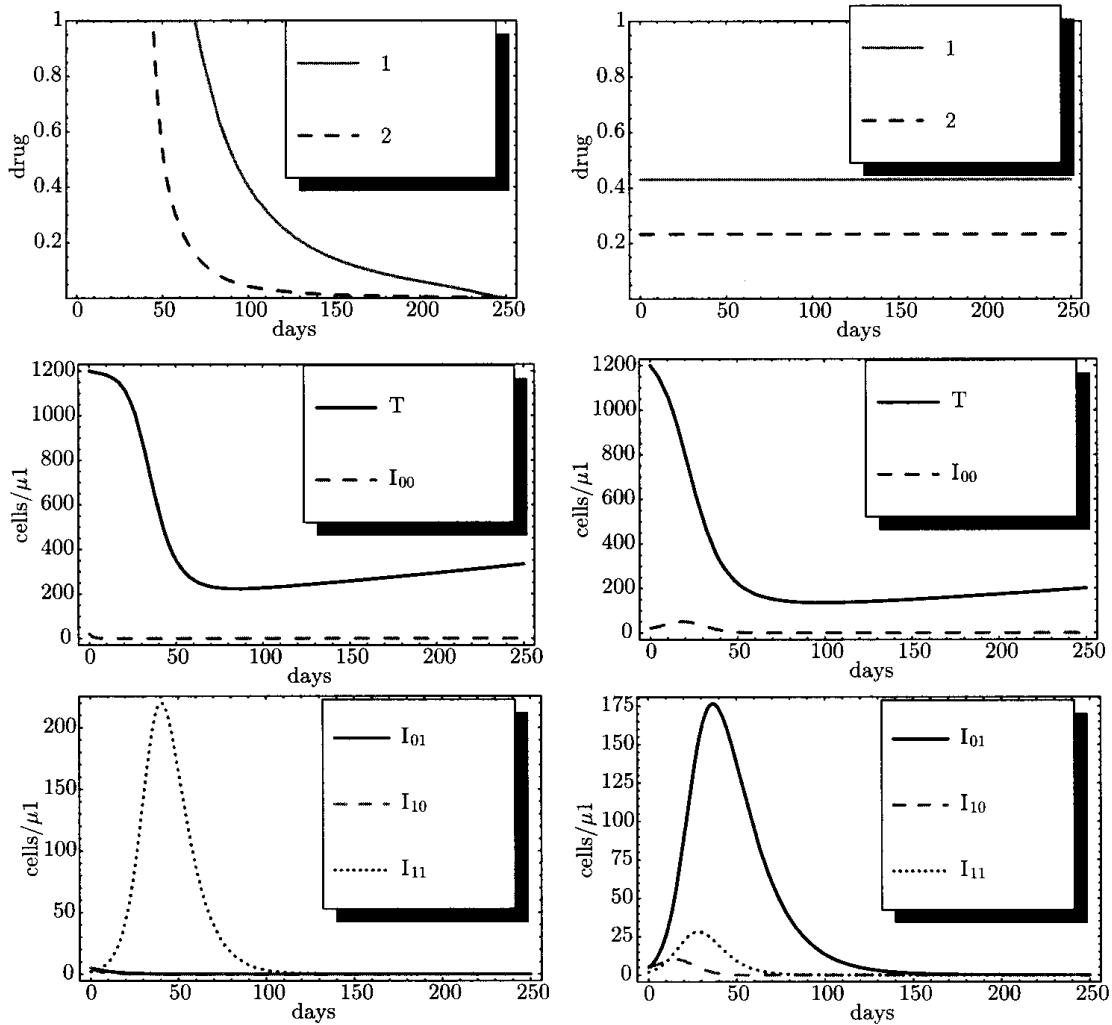


FIGURE 2. Comparison of healthy and infected T cell populations when optimal dosing is substantially better than constant dosing. Uninfected T cells are represented by  $T$ , T cells infected with wild-type virus by  $I_{00}$ , those infected with virus with type 1 mutations by  $I_{01}$ , infected with virus with type 2 mutations by  $I_{10}$ , and infected with virus with both types of mutations by  $I_{11}$ . Graphs on the left correspond to drug dosing computed using optimal control; those on the right correspond to constant drug dosing.

we incorporate into the transition rate constants) provides an extra benefit for the objective, and thus an advantage for “front-loaded” drug doses.

It is our belief that the intermediate equilibrium achieved around day 80 in Figure 3 for  $\eta_1$  is a phenomenon related to convergence. Our computational limitations prevented us from achieving further iterations in this example, but we plan to pursue further resources to explore this question. In particular, a more refined numerical optimal solution may yield significant improvement over constant drug dosing.

Because the behavior of the graphs varies greatly if parameter values are varied, we computed optimal control solutions for multiple different combinations of

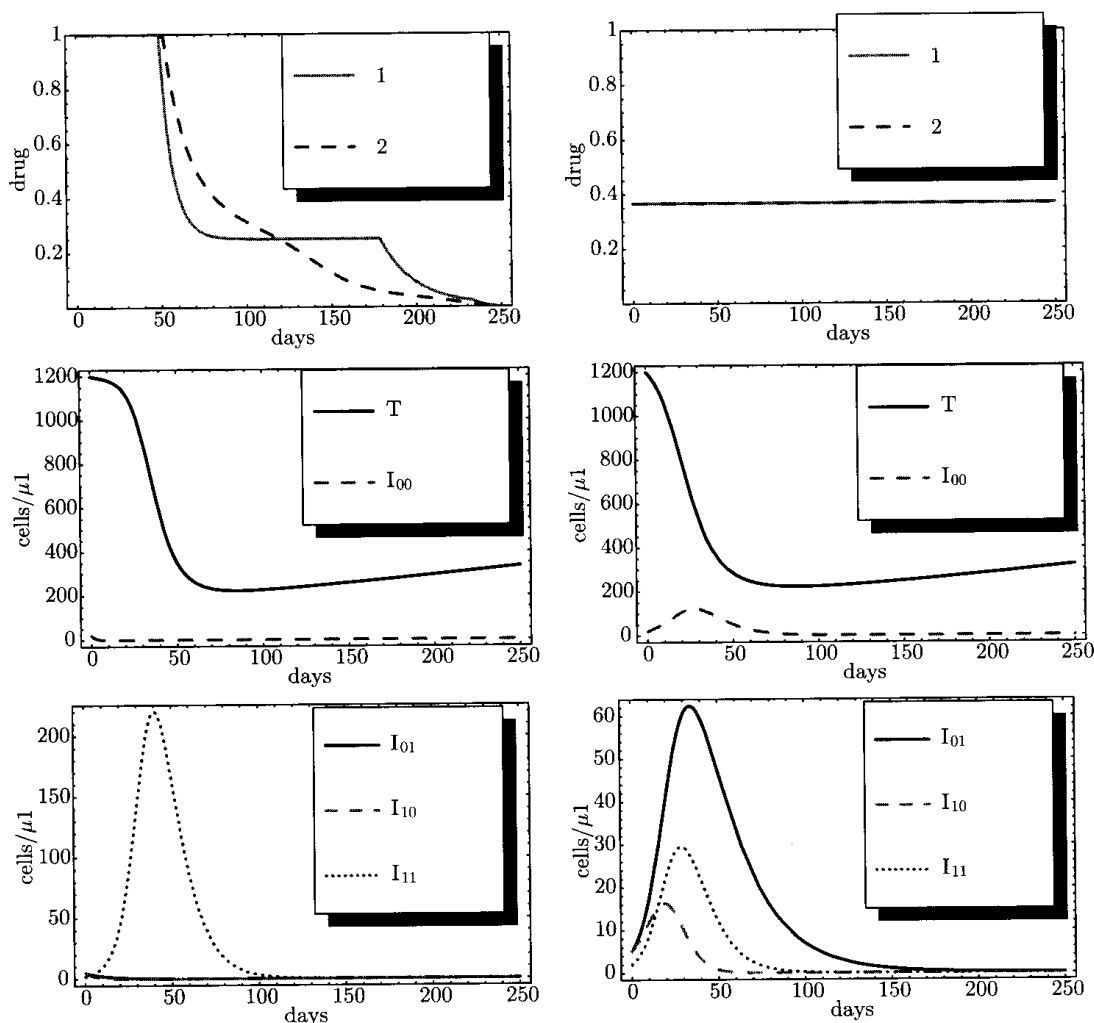


FIGURE 3. Comparison of healthy and infected T cell populations when optimal dosing is comparable to constant dosing. Uninfected T cells are represented by  $T$ , T cells infected with wild-type virus by  $I_{00}$ , those infected with virus with type 1 mutations by  $I_{01}$ , infected with virus with type 2 mutations by  $I_{10}$ , and infected with virus with both types of mutations by  $I_{11}$ . Graphs on the left correspond to drug dosing computed using optimal control; those on the right correspond to constant drug dosing.

TABLE 2. Parameter values used in Figures 2 and 3.

Graph	$\delta_{00}$	$w_{00}$	$w_{01}$	$w_{10}$	$w_{11}$	$B_1$	$B_2$
Figure 2	0.45	0.00001	0.0001	0.0001	0.01	10	50
Figure 3	0.4	0.0001	0.001	0.001	0.1	100	200

parameter values. The numerical results shown in this section are representative of the qualitative behaviors observed for different combinations of parameter values. We found substantial effects on the optimal solution curves due to changes

in  $\delta_{00}$  alone, as well as similar substantial effects due to changes only in the weights. Figure 3 shows the combination of these comparable effects.

## 6. Discussion and conclusions

In this paper, we introduced and analyzed optimal control treatments for a model of HIV with three different types of resistance to two drug classes. We showed existence and local uniqueness of optimal control solutions, and numerically calculated solution curves and the resulting cell population levels. We found that, in certain parameter regimes, the use of optimal control to determine dosing could yield substantially better health of a patient in comparison to constant-dose regimens that use the same total amount of drug. We found other parameter regimes in which there appeared to be no substantial benefit in using optimal control to determine dosing. Further computing resources are needed to compute optimal control solutions for longer time periods for the model we used here, but we feel this is a direction worth pursuing. In particular, it would be interesting to know if the T cell population with doubly-resistant virus is always favored early in the optimal dosing treatment period, and what happens to this population over longer treatment periods. Numerical analysis of any steady-state optimal solution may be helpful in addressing these issues as well.

The results represented in Figures 2 and 3 lead us to pose the following important problem: classify the settings in which variable-dose drug regimens determined by optimal control methods lead to significantly better outcomes than comparable constant-dose regimens. The solution may depend on the structure of the mathematical model, which can depend on properties of the disease being modeled. The solution certainly depends on the values of parameters used in the model. The form of the objective functional and the weights on its terms may play a substantial role in the answer. The result for certain models may also depend on the length of the treatment window. A criterion that is easy to compute for a given mathematical model of a disease would be highly desirable, to determine which models and parameter regimes would benefit significantly from the use of optimal control to compute patient drug doses. Even a criterion that gave uncertain, but highly likely, classification could be of great use.

Given the mixed results we found, and the additional limitation that a mathematical approximation of a disease cannot be completely accurate, we urge careful validation against test data before implementing drug doses for patients based on optimal control. Previous qualitative results have given useful ideas for experimental testing, such as the “Hit early, hit hard” results of Kirschner, Lenhart, and Serbin [12] and Fister, Lenhart, and McNally [7] for HIV chemotherapy. The model and the parameter regimes analyzed in [12] lead to substantial improvement in patient outcome when treatment regimens based on optimal control are used, in comparison to comparable constant-dose regimens. We feel it is valuable to continue such work on specific disease models that are likely to yield substantial improvements in outcome for current patients. However, we also advocate the theoretical examination of settings in which optimal control is likely to lead to better outcomes. Such an examination could be of broad benefit for future patients with HIV and other diseases for which it is possible to apply optimal control to such a mathematical model.

## References

- [1] S. Bonhoeffer, R. M. May, G. M. Shaw, M. A. Nowak, Virus dynamics and drug therapy, *Proc. Natl. Acad. Sci. USA* **94** (1997), 6971-6976.
- [2] S. Bonhoeffer and M. Nowak, Pre-existence and emergence of drug resistance in HIV-1 infection, *Proc. R. Soc. Lond. B* **264** (1997), 631-637.
- [3] S. Bonhoeffer, M. Rembiszewski, G. Ortiz, and D. Nixon, Risks and benefits of structured antiretroviral drug therapy interruptions in HIV-1 infection, *AIDS* **14** (2000), 2313-2322.
- [4] R. J. De Boer and C. A. B. Boucher, Anti-CD4 therapy for AIDS suggested by mathematical models, *Proc. R. Soc. Lond. B* **263** (1996), 899-905.
- [5] S. G. Deeks and B. D. Walker, The immune response to AIDS virus infection: good, bad, or both?, *J. Clin. Invest.* **113** (2004), 808-810.
- [6] P. Essunger and A. S. Perelson, Modeling HIV infection of CD4<sup>+</sup> T-cell subpopulations, *J. Theor. Biol.* **170** (1994), 367-391.
- [7] K. R. Fister, S. Lenhart and J. S. McNally, Optimizing chemotherapy in an HIV model, *Electron. J. Diff. Eq.* **32**, 1-12.
- [8] W. H. Fleming and R. W. Rishel, *Deterministic and Stochastic Optimal Control* (1975), Springer-Verlag, New York.
- [9] S. D. W. Frost and A. R. McLean, Quasispecies dynamics and the emergence of drug resistance during zidovudine therapy of HIV infection, *AIDS* **8** (1994), 323-332.
- [10] J. Goudsmit, A. De Ronde, D. D. Ho, and A. S. Perelson, Human immunodeficiency virus fitness in vivo: calculations based on a single zidovudine resistance mutation at codon 215 of reverse transcriptase, *J. Virol.* **70** (1996), 5662-5664.
- [11] Jung, E., S. Lenhart and Z. Feng (2002). Optimal control of treatments in a two-strain tuberculosis model. *Discrete Contin. Dyn. Syst. Ser. B* **2**, 473-482.
- [12] D. Kirschner, S. Lenhart, and S. Serbin, Optimal control of the chemotherapy of HIV, *J. Math. Biology* **35** (1997), 775-792.
- [13] D. Kirschner and G. F. Webb, Resistance, remission, and qualitative differences in HIV chemotherapy, *Emerg. Infect. Dis.* **3** (1997), 273-283.
- [14] L. M. Mansky and H. M. Temin, Lower in vivo mutation rate of human immunodeficiency virus type 1 than that predicted from the fidelity of purified reverse transcriptase, *J. Virol.* **69** (1995), 5087-5094.
- [15] A. R. McLean, V. C. Emery, A. Webster, P. D. Griffiths, Population dynamics of HIV within an individual after treatment with zidovudine, *AIDS* **5** (1991), 485-489.
- [16] A. R. McLean and M. A. Nowak, Competition between zidovudine sensitive and resistant strains of HIV, *AIDS* **6** (1992), 71-79.
- [17] H. Mohri, A. Perelson, K. Tung, R. Ribeiro, B. Ramratnam, M. Markowitz, R. Kost, A. Hurley, L. Weinberger, D. Cesar, M. Hellerstein, and D. Ho, Increased Turnover of T Lymphocytes in HIV-1 Infection and Its Reduction by Antiretroviral Therapy, *J. Exp. Med.* **194** (2001), 1277-1287.
- [18] H. Moore and W. Gu, A mathematical model for treatment-resistant mutations of HIV, *Math. Biosci. Eng.* **2** (2005), 363-380.
- [19] H. Moore and N. K. Li, A mathematical model for chronic myelogenous leukemia (CML) and T cell interaction, *J. Theor. Bio.* **227** (2004), 513-523.
- [20] A. U. Neumann, N. P. Lam, H. Dahari, D. R. Gretch, T. E. Wiley, T. J. Layden, A. S. Perelson, Hepatitis C viral dynamics in vivo and the antiviral efficacy of interferon-alpha therapy, *Science* **282** (1998), 103-107.
- [21] M. A. Nowak, S. Bonhoeffer, A. M. Hill, R. Boehme, H. C. Thomas, and H. McDade, Viral dynamics in hepatitis B virus infection, *Proc. Natl. Acad. Sci. U.S.A.* **93** (1996), 4398-4402.

- [22] M. A. Nowak, S. Bonhoeffer, G. M. Shaw, and R. M. May, Anti-viral drug treatment: dynamics of resistance in free virus and infected cell populations, *J. Theor. Biol.* **184** (1997), 203-217.
- [23] M. A. Nowak, and R. M. May, *Virus Dynamics: Mathematical Principles of Immunology and Virology* (2000), Oxford University Press, Oxford, UK.
- [24] A. S. Perelson, P. Essunger, Y. Cao, M. Vesanen, A. Hurley, K. Saksela, M. Markowitz, and D. D. Ho, Decay characteristics of HIV-1-infected compartments during combination therapy, *Nature* **387** (1997), 188-191.
- [25] A. S. Perelson, and P. W. Nelson, Mathematical analysis of HIV-I dynamics in vivo, *SIAM Review* **41** (1999), 3-44.
- [26] A. S. Perelson, A. U. Neumann, M. Markowitz, J. M. Leonard, and D. D. Ho, HIV-1 dynamics in vivo: virion clearance rate, infected cell life-span, and viral generation time, *Science* **271** (1996), 1582-1586.
- [27] L. S. Pontryagin, V. G. Boltyanskii, R. V. Gamkrelidze and E. F. Mishchenko, *The Mathematical Theory of Optimal Processes* (1962), Wiley, New Jersey.
- [28] D. D. Richman, D. Havlir, J. Corbeil, D. Looney, C. Ignacio, S. A. Spector, J. Sullivan, S. Cheeseman, K. Barringer, D. Pauletti, C. Shih, M. Myers, and J. Griffin, Nevirapine resistance mutations of human immunodeficiency virus type 1 selected during therapy, *J. Virol.* **68** (1994), 1660-1666.
- [29] N. I. Stilianakis, C. A. B. Boucher, M. D. De Jong, R. Van Leeuwen, R. Schuurman, and R. J. De Boer, Clinical data sets of human immunodeficiency virus type 1 reverse transcriptase-resistant mutants explained by a mathematical model, *J. Virol.* **71** (1997), 161-168.
- [30] UNAIDS, *UNAIDS/WHO AIDS Epidemic Update: December 2005*, <http://www.unaids.org/Epi2005/doc/report.html>.
- [31] L. M. Wein, R. M. D'Amato, and A. S. Perelson, Mathematical analysis of antiretroviral therapy aimed at HIV-1 eradication or maintenance of low viral loads, *J. Theor. Biol.* **192** (1998), 81-98.
- [32] L. M. Wein, M. Zenios, and M. A. Nowak, Dynamic multidrug therapies for HIV: a control theoretic approach, *J. Theor. Biol.* **185** (1997), 15-29.
- [33] R. A. Weiss, How does HIV cause AIDS?, *Science* **260** (1993), 1273-1279.
- [34] J. E. Wigginton, and D. Kirschner, A model to predict cell-mediated immune regulatory mechanisms during human infection with *Mycobacterium tuberculosis*, *J. Immunol.* **166** (2001), 1951-1967.

DEPARTMENT OF MATHEMATICS, HARVEY MUDD COLLEGE, CLAREMONT, CA 91711  
E-mail address: [gu@math.hmc.edu](mailto:gu@math.hmc.edu)

AMERICAN INSTITUTE OF MATHEMATICS, 360 PORTAGE AVENUE, PALO ALTO, CA 94306  
E-mail address: [moore@aimath.org](mailto:moore@aimath.org)